Growth and electron quantization of metastable silver films on Si(001)

Iwao Matsuda,[1] Han Woong Yeom,[2,*] Takehiro Tanikawa,[3] Kensuke Tono,[1] Tadaaki Nagao,[3] Shuji Hasegawa,[3] and Toshiaki Ohta[1]

[1]*Department of Chemistry, The University of Tokyo, Hongo, Tokyo 113-0033, Japan*

[2]*Atomic-Scale Surface Science Research Center and Institute of Physics and Applied Physics, Yonsei University, Seoul 120-749, Korea*

[3]*Department of Physics, The University of Tokyo, Hongo, Tokyo 113-0033, Japan*

(Received 9 August 2000; published 13 March 2001)

The growth morphology and the electronic structures of thin metastable Ag films grown on the Si(001)2 $\times$1 surface at low temperatures are investigated by scanning tunneling microscopy and angle-resolved photoemission spectroscopy using synchrotron radiation. The morphology of Ag films exhibits a strong thickness and temperature dependence indicating an intriguing growth mechanism. The as-deposited film at $\sim$100 K is composed of nanoclusters with flat tops in a uniform quasi-layer-by-layer film at 2–3 ML and of homogeneous clusters having more three-dimensional (3D) character above $\sim$5 ML. By subsequent annealing at 300–450 K, flat epitaxial Ag(111) films are formed at a nominal coverage larger than 5 ML, while a percolating network of 2D islands is formed at a lower coverage. For the optimally annealed epitaxial films, discrete Ag 5*s* states are observed at binding energies of 0.3–3 eV together with the Ag(111) surface state. The discrete electronic states are consistently interpreted by a standard description of the quantum-well states (QWS's) based on phase-shift quantization. No such well-defined QWS is observed for the films with a coverage less than $\sim$5 ML. The phase shift, the energy dispersion, and the thickness-versus-energy relation of the QWS's of the epitaxial Ag(111) films are consistently derived. The QWS's in photoemission spectra show two distinctive types of the photon-energy dependence in their binding energies; the oscillatory shifts for $h\nu = 5-15$ eV and no such shift at $h\nu = 20-25$ eV. This can be explained in terms of the different final states in the photoemission process.

DOI: 10.1103/PhysRevB.63.125325 PACS number(s): 73.90.+f, 79.60.Dp

I. INTRODUCTION

The quantum-well states (QWS's) associated with the electron confinement in a nanometer scale have attracted considerable interest due to their importance in low-dimensional physics and in the magnetic/electronic-device applications. A well-known example is the QWS in semiconductor/semiconductor-layered systems, which are relevant to the optoelectronic devices.[1,2] Recently many investigators have focused on the QWS's in metal/metal systems, which show the oscillatory magnetic coupling and the giant magnetoresistance.[3–6] On the other hand, the QWS's in the metal/semiconductor systems have received relatively little attention due partly to the difficulty of growing epitaxial metal films on the semiconductor substrates. However, recent scanning tunneling microscopy (STM) and low-energy electron diffraction (LEED) studies have found that continuous and atomically flat Ag(111) films can be formed on the semiconductor substrates such as GaAs(110),[7,8] Si(111),[9,10] and Si(001).[11,12] Such films are prepared when Ag is deposited at a sufficiently low temperature of $<$130 K and a mild annealing up to 300–400 K follows. This unique growth procedure (the so-called ''two-step growth'') makes it possible to study the QWS's of metal/semiconductor systems in a well-controlled and systematic manner.

On the other hand, the growth mechanism of such a metastable epitaxial Ag film itself has received a great deal of interest, which features an interesting critical behavior in the film thickness. The Ag films are shown to have a magic thickness of $\sim$6 ML where the films have the lowest energy.[7,9] While a newly developed theoretical growth model (the so-called ''electronic growth'' model) invoked an important role of the QWS's within the films,[13] a direct experimental study of the electronic structures of such films has been lacking. Furthermore much complex growth morphology has been identified for the Ag metastable films on a Si(111)7$\times$7 surface below the critical thickness, which cannot easily be explained within the simple electronic-growth model.[14] This situation obviously requests a detailed electronic-structural study for the metastable epitaxial films grown on a semiconductor substrate through the two-step growth process.

Angle-resolved photoelectron spectroscopy (ARPES) is a unique direct probe to the electronic structures of thin films. This tool has successfully revealed the presence and the physical properties of the QWS's on various metal thin films.[3–6,15–25] An early ARPES study of the Ag films grown on Si(111) at room temperature has identified very weak QWS features[19] although later STM studies showed that such a film at room temperature is far from an ideal epitaxial film.[26] Later ARPES studies clearly observed QWS's for the Ag(111) films on GaAs(110) grown by the low-temperature two-step process.[15,16] However, without the morphological study of the Ag films on GaAs(110), Neuhold and Horn originally interpreted the QWS as due to the Ag islands and thus no direct correlation with the film morphology could be obtained.[15,16] A very recent ARPES study also observed well-defined QWS's for the Ag(111) films grown on Si(111) in a similar way but no detailed discussion of the QWS's was provided.[10]

In this paper, we report on a study of the QWS's and the growth morphology of the metastable Ag(111) films grown epitaxially on the Si(001)2$\times$1 surface by the two-step process, that is, Ag deposition at $\sim$100 K and subsequent an-

nealing at 300–500 K. For a wide temperature and thickness range, the film-growth mode was surveyed by LEED and reflection high-energy electron diffraction (RHEED). Using STM, the film morphology was investigated in detail at two representative Ag coverages of 2.5 and 5 ML, where significantly different types of the morphology are observed. The electronic structures of the Ag films were investigated by ARPES using synchrotron radiation for thickness up to 30 ML. The well-defined QWS's were identified clearly at the Ag film thickness of 5–30 ML. The physical properties of the QWS's are studied in detail and are analyzed using the well-established phase-shift quantization rule.[18,21–25] The correlation between the film structure and the QWS's are discussed.

II. EXPERIMENTS

The STM and ARPES experiments are preformed in two different locations. For the STM measurement, we used a commercial ultrahigh vacuum low-temperature STM (UNISOKU USM501 type) equipped with RHEED system.[27] The base pressure in the chamber was 7×10^{-11} Torr. All the STM images were taken in the constant-current mode at 65 K. The ARPES measurements were performed using synchrotron radiation on the vacuum ultraviolet ($h\nu=5-40$ eV) beam line BL-7B (Research Center for Spectrochemistry, the University of Tokyo) at Photon Factory, Japan.[28] It is equipped with an angle-resolved photoelectron spectrometer (ADES 400, Vacuum Generator), a LEED optics, a quartz crystal thickness monitor, and a sample manipulator with a cryostat.[29–32] The base pressure of this system was $\sim1\times10^{-10}$ mbar during the experiment. The overall angular and energy resolutions chosen were $\sim1.5°$ and ~0.1 eV, respectively. Linearly-polarized synchrotron radiation was incident at an angle (θ_i) of 45° from the surface normal along the [110] axis of the Si(001) crystal. All the ARPES spectra were measured at 120 K and at a polar emission angle θ_e of 0°. Each spectrum is taken at $h\nu=21$ eV and is normalized to the intensity above the Fermi level E_F, which is proportional to the incident photon flux.

A Si(001) substrate was first prepared by the *ex situ* chemical etching and then a clean Si(001)2×1 surface, as checked by RHEED and STM, was prepared by stepwise degassing and finally by flash annealing at 1500 K. Ag was deposited onto the Si(001)2×1 surface held at 65 K or at 120 K using a W filament (in the STM apparatus) or a graphite-effusion cell (in the ARPES system). The film thickness in the present study is given in terms of the monolayers of an Ag(111) atomic layer (1.39×10^{15} atoms/cm^2), which was determined from the evaporation rate of the source as calibrated by the well-known phase diagram of the room-temperature Ag adsorption on Si(001)2×1 (Refs. 30–33) and by a quartz microbalance.

III. RESULTS AND DISCUSSION

A. Growth morphology at low temperature: An STM study

Figure 1(a) shows an STM image for the Si(001) surface with 2.5 ML Ag deposited at 65 K. We can observe a granular Ag film composed of nanoclusters in quite a uniform-size distribution of 20–30 Å, which evenly covers the whole surface. A line profile of several such clusters [the *A-B* line in Fig. 1(a)], shown in Fig. 1(b), exhibits that the Ag nanoclusters have flat tops with sharp edges indicating their 2D character. Within our experimental resolution, the nanoclusters likely have uniform height differences of ~2.6 Å that may correspond to the height of one Ag(111) layer (2.36 Å). Hence, Ag grows on Si(001)2×1 at 65 K in a quasi-layer-by-layer manner at this coverage range although the film is composed of nanoclusters formed by the limited diffusion of Ag adsorbates. A recent LEED study observed a clear LEED intensity oscillation during the Ag growth on Si(001)2×1 at 130 K,[12] which is consistent with this interpretation. Our own RHEED measurements also showed a clear oscillation of the (00)-spot intensity indicating this quasi layer-by-layer growth. Such a quasi-layer-by-layer growth is also reported for the growth of Ag on Si(111)7×7 at 90–150 K by STM (Ref. 34) and RHEED.[35] Indeed, the STM image of the Ag films of 2.5 ML grown on Si(111)7×7 at 90 K is almost identical to the present result on Si(001).[34]

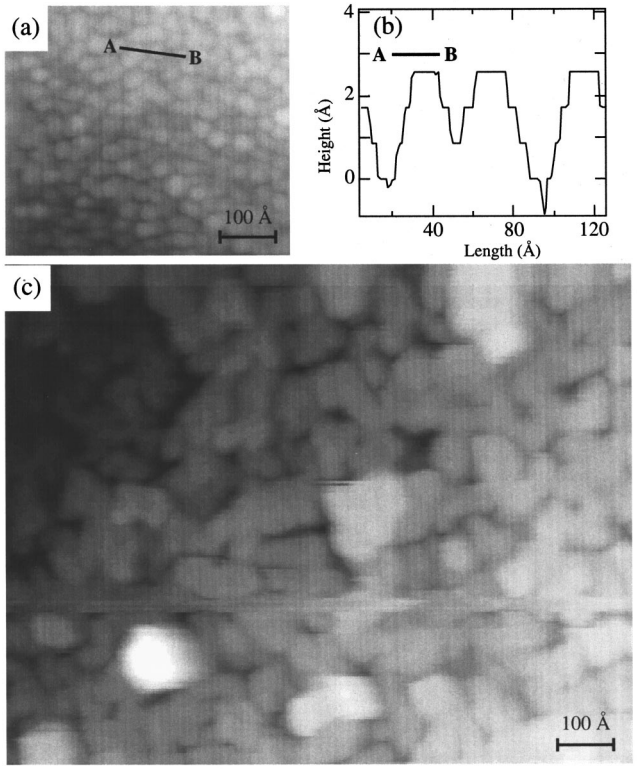

FIG. 1. (a) An STM image for the 2.5-ML Ag deposition on a Si(001)2×1 surface at 65 K. The image was taken at a tip bias voltage of 5.0 V. (b) A line profile of the *A-B* line in (a). (c) A similar STM image for the same surface after annealing at 300 K for 1 h.

For the Ag deposition of 5 ML at 65 K, the nanoclusters grow in their lateral size (30–40 Å) and height [Fig. 2(a)]. A line profile [*C-D* line of Fig. 2(a)] shows that the nanocluster shape is apparently different from those of 2.5 ML. They have sharp tops instead of flat ones and no discrete edges. This indicates that the islands start to have a 3D feature,

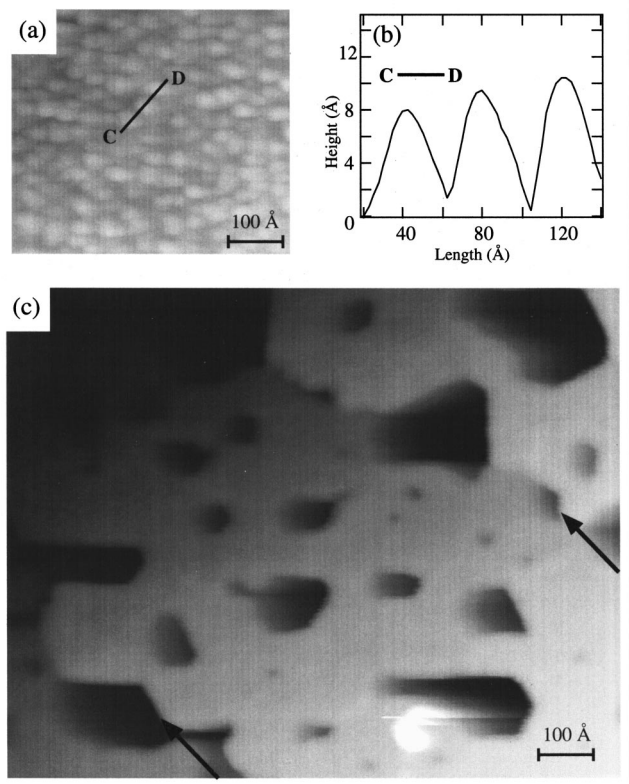

FIG. 2. (a) An STM image for the 5-ML Ag deposition on a Si(001)2×1 surface at 65 K taken at a tip bias voltage of 3.0 V. (b) A line profile of the *C-D* line in (a). (c) A similar STM image for the same surface after annealing at 300 K for 1 h.

which can be related to the damping of the intensity oscillations in the previous LEED study[12] and in our RHEED study, upon the coverage increase. Thus, the present STM results confirm that the low-temperature Ag growth on Si(001) occurs in a quasi layer-by-layer manner, as reported by Horn-von Hoegen *et al.*[12] and is also similar to the Ag low-temperature growth on Si(111).[34] However, the kinetic roughening of the growth front occurs to have more 3D character upon the increase of the film thickness.

As previously reported for Ag films on GaAs(110) and Si(111), the morphology of these low-temperature grown films is only metastable and it changes drastically by mild annealing at 300–400 K. As shown in Fig. 1(c) for the 2.5-ML Ag film on Si(001), after annealing at 300 K for 1 h, a more or less irregular surface feature is found. The film is a percolated network of 2D, atomically flat, islands of roughly ~100 Å in their lateral size. The height of the 2D islands is, however, not that uniform with zero, one, two, three, or even four atomic layers: roughly 60% of the whole islands have the height of two or three atomic layers. This STM image is similar to those for the Ag films of the same coverage on Si(111)7×7 prepared in a similar procedure.[9,14] However, it can be noted that the Ag 2D islands on Si(001) has a much weaker tendency to prefer a single height of 2 ML in contrast to those on Si(111).[9,14] It is not certain in this stage as to what is the origin of this difference, with many possible factors such as the different substrate surface structures or the subtle difference in the growth conditions.

The film morphology after annealing at 300 K exhibits yet another characteristic feature as shown in Fig. 2(c). In sharp contrast to the annealed film of 2.5 ML [Fig. 1(c)], an atomically flat Ag film is formed over the whole surface at the nominal coverage of 5 ML. The film features the steps (indicated by arrows in the figure) and also the ''pit holes'' (dark spots or areas in the image). The steps are identified as due to those of the Si(001) substrate by comparing with the step morphology (such as the orientation and separations) of the clean Si(001) surface before the evaporation. That is, a flat Ag film is formed on each terrace of Si(001) substrate without altering the substrate steps significantly. This is also confirmed in the previous STM studies.[11,12] As identified by RHEED and LEED, the Ag film is a well-ordered epitaxial Ag(111) film. The most startling feature of the film is apparently the pit holes. It is likely that the pit holes reach down to the Si substrate as in the very similar cases of the Ag epitaxial films on GaAs(110) (Refs. 7, 8) and Si(111) (Ref. 9) grown in identical procedures. We are then able to estimate the critical thickness of the Ag film from the surface area of the pit holes and the nominal coverage of the deposited Ag. This estimation yields a critical thickness 6 ML, which is the same as reported previously for Ag/GaAs(110) (Ref. 7) and Ag/Si(111).[9]

This result generally favors the idea of electronic growth proposed by Zhang and co-workers[13] that the Ag film is most stable at the thickness of ~5 ML, being insensitive to the strain energy imposed by the substrate due to the prevailing contribution of the quantized electrons within the film. However, as shown for Si(001) and also for Si(111) recently,[9,14] the Ag films on Si surfaces at a lower coverage of 2–3 ML do not share the growth morphology with a critical thickness of 6 ML, in contrast to that on GaAs(110).[7,8] On the Si(111) surface, the Ag film exhibits another critical thickness of 2 ML, i.e., a strong preference of 2-ML single-height 2D islands at a coverage of less than 3 ML.[14] Zhang and his coworkers recently argued that this is also consistent with their own electronic-growth model, but it was not clear at all why there should be two different critical thicknesses of 2 ML and 6 ML for the Ag films on Si(111).[13,14] As we have shown here, the Ag growth on Si(001) at a lower coverage than 6 ML does not follow the expectation of the electronic-growth model and does not exhibit another critical coverage of 2 ML. While further studies and discussion are greatly required to understand this intriguing growth mode and its dependence on the surface structures, it seems obvious that the electronic-growth model oversimplifies the difference of various substrate surface structures.

B. Electronic states of the Ag films: An ARPES study

An approach to understand the intriguing growth morphology and the role of quantized electronic states can apparently be to study the electronic states of the films directly by ARPES. Figure 3 shows the normal-emission ARPES spectra for the Ag film with a nominal thickness of 14 ML grown on Si(001) at 120 K and similar spectra also for the

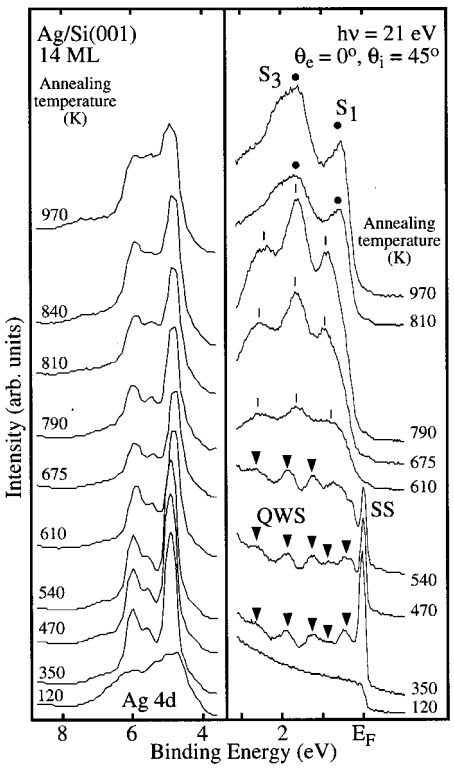

FIG. 3. A collection of normal-emission ARPES spectra for the Si(001)2×1 surface with 14-ML Ag deposited at 120 K and subsequently annealed at various temperatures indicated for 1 min. The spectra are taken at the photon energy of 21.0 eV and at the photon incident angle θ_i with respect to the surface normal of 45°. See text for the assignments of the peaks in the spectra.

same film but after annealing at different temperatures for a minute. Each spectrum is taken at a photon energy ($h\nu$) of 21.0 eV. The strong emissions at a binding energy E_B of 5–6 eV are the emissions from the Ag $4d$ states. The differences of the ARPES spectra clearly indicate the drastic change of the electronic structure of the Ag film by the annealing. Without the annealing, the spectral shape of Ag $4d$ is very broad with many possible components and the valence band near E_F is featureless (indicated as 120 K in Fig. 3). This spectral shape is similar to those of Ag deposited on Si(001)2×1 at room temperature with a coverage larger than 3 ML, indicating the formation of rather disordered Ag clusters.[32] The formation of such clusters for the low temperature (LT) deposition is consistent with our STM in Fig. 2(c) and the previous LEED results.[12] After annealing at 300–350 K, we observed clear (1×1) LEED and RHEED patterns of Ag(111), which is also consistent with the previous STM and LEED studies, as discussed above.[11,12] The ARPES spectra after annealing show an intense structure just below E_F (denoted as SS) and the fine peaks at the binding energies E_B of 0.3–3 eV. In addition, the Ag $4d$ has well-defined structures after the annealing at 350 K (Fig. 3). Through the comparison with the ARPES studies of a clean Ag(111) surface[36] and of the epitaxial Ag(111) films[18,24,25] SS can unambiguously be assigned to the surface state of the Ag(111) surface layer. As rigorously interpreted below and also through the comparison with previous ARPES studies of the Ag(111) thin films,[10,15,16,24,25] the fine peaks (the filled triangles) at E_B of 0.3–3 eV are identified as the QWS's. In this case, the electrons are confined by the 1D potential well along the normal to the film, which is formed by the vacuum/Ag and the Ag/Si interfaces. This will be discussed in detail below.

With the further annealing at 400–540 K, the Ag(111) surface state gradually perishes while the QWS's and the Ag $4d$ states remain more or less intact. At this temperature range no significant change of LEED patterns was observed. However, above ~600 K, the surface state and the QWS's all vanish and are replaced by three distinctive peaks at E_B ~0.7, 1.6, and 2.5 eV. The LEED pattern, then, shows a mixture of the Ag(111)1×1 pattern and the Si(001)2×1 pattern. Above 800 K, the valence-band spectra is dominated by two strong peaks at E_B=0.5 and 1.5 eV, which are identified as due to the surface states of the Si(001)2×3-Ag surface[30] in consistency with the observation of a clear 2×3 LEED pattern. The surface after the annealing above 800 K is thus thought to be composed of the 2×3-Ag wetting layers [with a coverage of ~0.6 ML (Ref. 30)] and the large 3D Ag islands. The origins of the three peaks at intermediate temperature range (tick marks in Fig. 3) are not clear at all although the 2×1 LEED pattern observed at this coverage is likely due to the Si(001)2×1-Ag surface. The Si(001)2×1-Ag surface is typically formed for the room temperature adsorption of Ag at and above ~1.0 ML and is the wetting layer for the room-temperature Stranski-Krastanov growth of Ag on Si(001)2×1.[32] However the correlation of the three peaks with the surface states of 2×1-Ag (Ref. 32) is not obvious. In any case, it is clear that the epitaxial Ag layers formed by the two-step procedure are only metastable. The annealing above ~550 K converts the Ag films gradually into the conventional Stranski-Krastanov type morphology of the 2D wetting layers (the 2×3-Ag layer) with the 3D islands. It is interesting to note that the Ag(111) surface states (SS in Fig. 3) start to be depopulated at a lower temperature than that at which the QWS's are affected by the annealing. We can speculate that the topmost layer of the epitaxial film is more sensitive to the annealing than the whole film. This is natural since the mass transport from the epitaxial layers to the Ag 3D islands is likely to occur from the topmost layers. Otherwise, this intriguing temperature dependence of the surface state might be related to the effect of the film strain as recently suggested for the Ag(111) films on Si(111).[10] The QWS's and the surface states are then a qualitative criterion of the perfection of the film and of the order of the surface layer, respectively. In adopting this criterion and also from the LEED study, we can conclude that the Ag film after the annealing at 300–400 K has the best film and surface quality.

We then studied the QWS's of the Ag films after annealing at 300–400 K for different Ag film thicknesses of up to 30 ML. In Fig. 4, a series of ARPES spectra in the energy range from E_F to the lower-binding energy tail of the Ag $4d$ level is shown for the epitaxial Ag films after annealing with various thickness (the nominal coverages are given). At the coverages of 0.3 and 0.5 ML, we find three peaks, S, B_1, and B_2, which are identified as due to the Si(001) substrate. At

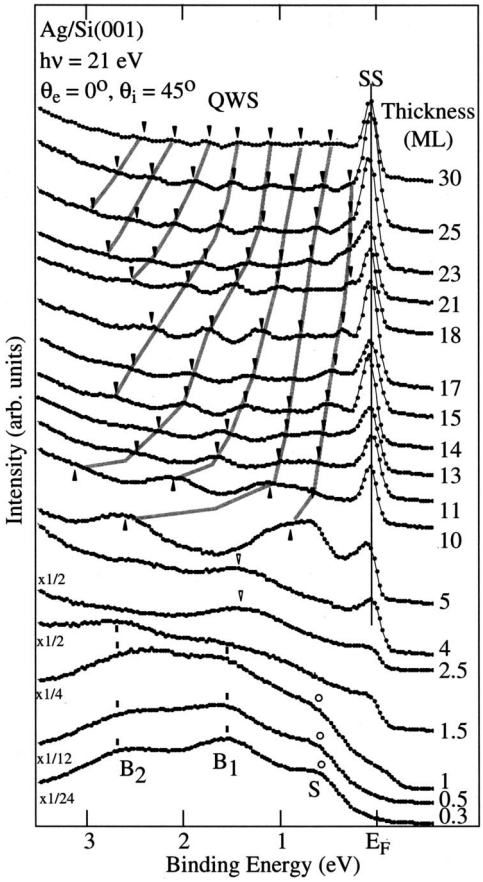

FIG. 4. Normal-emission ARPES spectra for the Ag films of varying thickness on Si(001)2×1 formed by deposition at 120 K and subsequently, annealing at 300–400 K. The conditions of ARPES measurement are same as in Fig. 3. The peak positions of the quantum-well states are marked with filled symbols and are traced with gray lines. See text for more explanation of the different electronic states assigned.

1.0 ML, the density of states at E_F is observed, which is obviously due to the Ag film. This Fermi-edge emission is very clear at 1.5 and 2.5 ML with the decreasing intensity of the substrate contribution. From the coverage of 4 ML, the ARPES spectra exhibit the Ag(111) surface state mentioned above. This means that the film starts to have large flat surface areas with the structure of the Ag(111)1×1 surface. At higher coverage than 4 ML, the surface state develops further and the valence states, which are clearly different from those of the Si substrate states, are observed at the binding energies of 0.3–3.0 eV (the filled symbols in Fig. 4). These states are proved to be the QWS's of the Ag(111) films as explained below. It is worth noting that the QWS's and the surface state are not clearly identified for the films with the coverage of 2.5 ML. This might be related to the film morphology, as observed by the present STM study. That is, the films at <3 ML exhibit only the irregular 2D islands with various thickness of 1–4 layers while those at $\geqslant 5$ ML posses large atomically flat terraces with a well-defined height.

It should first be noted from our STM result [Fig. 2(c)] that the ARPES peaks at a nominal coverage of 5 ML correspond actually to the QWS's of a 6-ML-thick film. In Fig. 4, the systematic variation of the QWS binding energies are observed with respect to the film thickness, which is due to the change of the width of the quantum well.[15–25] In order to quantify the binding energies of QWS's, several models have been used in the previous studies.[3,5,6,15–25,37] We invoke the ''phase-shift quantization rule,'' which has been successfully applied to the interpretation of the image states and the surface states on clean metal surfaces and of the QWS in the metal thin films.[5,17–25] The quantization condition for the existence of a QWS is

$$\phi_{\mathrm{vac}}(E_n)+2k_{\perp}(E_n)d+\phi_{\mathrm{sub}}(E_n)=2\pi n, \tag{1}$$

where n is the quantum number, $k_{\perp}$ is the wave vector of the envelope function of a Bloch state perpendicular to the surface, and d is the film thickness. $\phi_{\mathrm{vac}}(E_n)$ and $\phi_{\mathrm{sub}}(E_n)$ are the phase shifts upon reflection at the two boundaries of the film towards the vacuum and towards the substrate, respectively. In Eq. (1), $k_{\perp}(E_n)$ represents the band dispersion along the normal to the Ag(111) surface (the Γ-L direction of the 3D Brillouin zone).[20,21,24] With a simple transformation of Eq. (1), one can derive the relationship of the thickness versus energy, the so-called ''structure plot,'' of the nth QWS,[20,21]

$$d_n(E_n)=[n-1+2\pi\phi_{\mathrm{vac}}(E_n)+2\pi\phi_{\mathrm{sub}}(E_n)]/[1-k_{\perp}(E_n)], \tag{2}$$

where d_n is given in the number of the Ag(111) atomic layers and $k_{\perp}(E)$ in the unit of the size of the zone-boundary wave vector at the L point.

In order to solve Eq. (2), it is required to know the dispersion relation of the Ag(111) *sp* band along the [111] direction, $k_{\perp}(E)$, and the energy dependence of the total phase shift at the two boundaries, $\phi_{\mathrm{tot}}(E)=2\pi\phi_{\mathrm{vac}}(E)+2\pi\phi_{\mathrm{sub}}(E)$. The dispersion $k_{\perp}(E)$ can be determined experimentally.[24] Briefly, if the nth quantum state for a film thickness d happens to have the same binding energy as that of n' ($n'=n+1$, for example) at a thickness of d', then the simultaneous solution of Eq. (1) for these two quantum states yields

$$k_{\perp}=\pi(n'-n)/(d'-d). \tag{3}$$

The $E(k_{\perp})$ data measured in this way from the present Ag(111) films is given in Fig. 5(a) as solid circles. The experimental dispersion is then fitted with a fitting function, which is based on the two-band nearly free electron model,

$$E(k_{\perp})=E_0-[ak_{\perp}^2+U-(4a^2bk_{\perp}^2+U^2)^{1/2}], \tag{4}$$

with $a=h^2/(8\pi^2m^*)$ and $b=3\pi^2/a_0^2$, $U=4.2$ eV the width of the band gap at the L point, and $E_0=0.31$ the position of the *sp*-band edge relative to E_F.[18,24] The fit gives the electron effective mass of this band, m^* as $0.78m_e$. In this method, the only source of experimental error is introduced by a possible difference between the nominal and measured film thickness. The uncertainty of the film-thickness measurement is ~10% in the worst case, which leads to the same ~10% error in the $k_{\perp}$ value determined. The standard deviation of the $E(k_{\perp})$ fit given above is 0.08 eV but is roughly three times larger when we consider the largest possible 10%

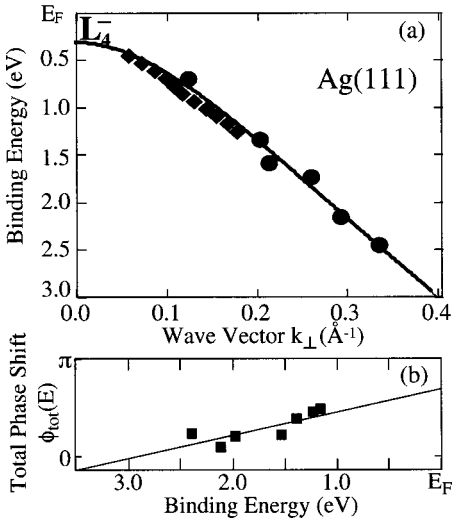

FIG. 5. (a) The *sp*-band dispersion for Ag bulk along the Γ-*L* Brillouin-zone line. Solid circles and diamonds are data points from the present experiment on Ag(111)/Si(001) and the previous reports on Ag(111)/Cu(111) (Ref. 25), respectively. The solid curve is a least-squares fit of the Ag/Si(001) data points based on the two-band nearly free-electron model (see text). (b) Change of the phase shift of the $n=4$ quantum-well state of Ag(111)/Si(001) with its binding energy. Experimental data and a least-squares fit are shown as solid squares and a solid line, respectively.

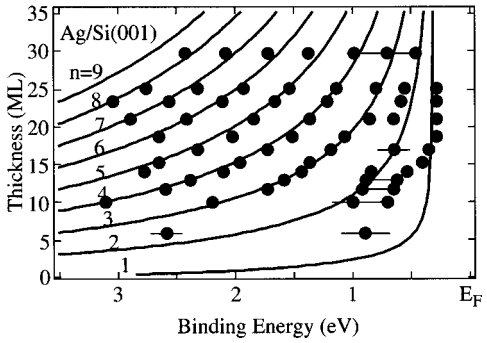

FIG. 6. Comparison between the model calculation based on the phase-quantization model (curves) and the experimental data (dots with the error bars) for the binding energies of the quantum-well states for the epitaxial Ag(111) films on Si(001) as a function of thickness. See text for the explanation of the model calculation.

uncertainly in $k_\perp$. Even in that worst case, however, m^* can accurately be determined within $0.005m_e$. This value is almost the same as those obtained by the identical method for the QWS's in Ag(111)/graphite(0001) (Ref. 18) and in Ag(111)/Cu(111) [given as solid diamonds in Fig. 5(a)].[24] The resulting dispersion curve is also in good agreement with the previous theoretical calculation of the bulk Ag metal.[36] What is left to solve Eq. (2) is now the total phase shift $\phi_{\rm tot}(E)$. The typical way to find the total phase shift reasonably is to assume that $\phi_{\rm tot}$ is a linear function of E (Refs. 20, 21) and to fit $\phi_{\rm tot}(E)$ by putting the d_n and E_n data measured for one of the QWS's, into Eq. (2).[20,21] We chose the $n=4$ QWS since this state is observed around the center of the observed energy range and at most of the coverages. As shown in Fig. 5(b), the phase shifts obtained for $n=4$ QWS's (solid squares) are fitted to $\phi_{\rm tot}(E)=(-0.25\pi\ {\rm eV}^{-1})E+0.71\pi$.

From the empirical bulk-band dispersion [Fig. 5(a)] and the total phase shift [Fig. 5(b)], the structure plots [Eq. (2)] for all the QWS's are calculated as shown in Fig. 6 together with the experimental energy positions of the QWS's obtained from Fig. 4. To the best of our knowledge, no preivous report is available for the structure plots of the QWS's in a metal film on a semiconductor substrate and of the QWS's of a Ag(111) film. The calculated energy positions of the QWS fit the experimental data reasonably well except for $n=1$ and $n=2$ QWS's with binding energies less than $\sim$1.0 eV. This deviation may be due to the change of the Ag band structure by most likely the strain induced by the Si(001) substrate or due to the limitation of the approximations used in obtaining the bulk dispersion and the total phase shift. As seen in Fig. 5, the phase shift at this energy range is chosen from the linear extrapolation of the energy vs phase shift relation, which is determined experimentally only at the energy of 1.0–2.5 eV. This indicates that there can be a possible difference in the phase shift between our estimation based on the simple, linear extrapolation and the reality in the energy region of <1 eV. This possibility becomes much more plausible when we consider the fact that the substrate Si valence-band maximum is located at $E_B\sim 0.6$ eV. That is, there might be a drastic difference in the phase shift at the Ag/Si interface between the energy regions inside and outside the substrate band gap making the QWS energy positions deviate from those expected from the above theoretical model. Quantitative information on the strain of such thin Ag films and further study on the phase shifts will be crucial to understand this issue.

Let us now turn back to the phase shifts at the two boundaries. A phase shift at the Ag-vacuum interface can be expressed as

$$\phi_{\rm vac}(E)=\pi[3.4/(E_v-E)]^{1/2}-\pi, \qquad (5)$$

which represents the phase shift for an image potential within the WKB approximation[38] and where E_v is the vacuum level. $\phi_{\rm vac}(E)$ at E_F can be evaluated by introducing the work function of the Ag(111) surface (4.5 eV) into (E_v-E) of Eq. (5), which yields $\phi_{\rm vac}(E_F)=-0.13\pi$. Since $\phi_{\rm int}(E_F)$ was evaluated to be $\sim 0.71\pi$ [Fig. 5(b)], one can estimate the value of $\phi_{\rm sub}(E_F)$ to be $\sim 0.84\pi$. Since E_F lies within the Si band gap, the electrons at E_F are Bragg-reflected at the Ag-Si interface, that is, $\phi_{\rm sub}$ should ideally be π. In spite of the crude approximations used, $\phi_{\rm sub}(E_F)$ of Ag(111)/Si(001) obtained above is close to this expectation. It contrast, the total phase shift of QWS's of a Ag(100) film on a metal substrate was reported to be -0.4π at E_F.[21] This clearly indicates that the metal/semiconductor and the metal/metal interfaces have large differences in the scattering of a Bloch-state electron near the Fermi level.[39]

Previously, it was reported that the QWS's in ARPES spectra exhibit a certain binding-energy shift with respect to the photon-energy variation.[25,40] This means that the above structure-plot analysis could be affected by the use of a dif-

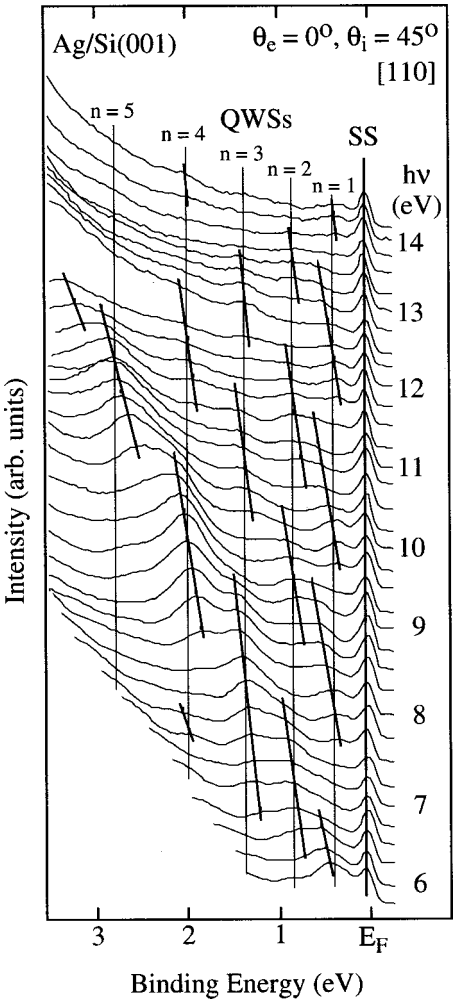

FIG. 7. Normal-emission ARPES spectra for the 14-ML-thick Ag(111) epitaxial film on Si(001) taken at photon energies ($h\nu$) of 5.75–14.25 eV. The step in photon energy is 0.25 eV. The thick lines are guides to the eye showing the peak motions of the quantum-well states. The thin lines indicate roughly the maximum-intensity position for each quantum-well states.

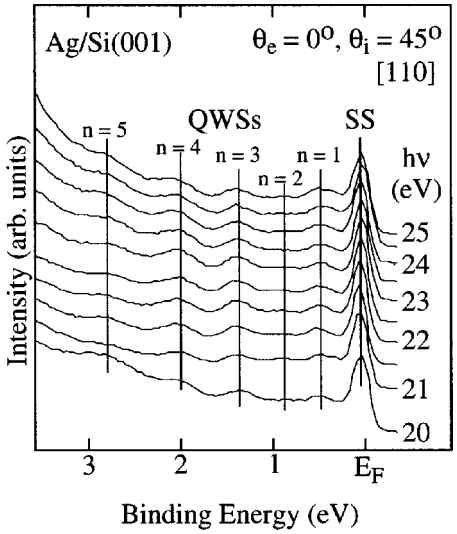

FIG. 8. Similar to Fig. 7 except that the photon energies are from 20 to 25 eV. The thin lines indicate the peak position of each quantum-well state.

ferent photon energy. We thus studied the photon-energy dependence of the ARPES spectra in detail. The spectra of the 14-ML film are shown in Figs. 7 and 8 for photon energies of 5.75–14.25 eV and 20–25 eV, respectively. Each spectrum is normalized by the intensity of the Ag(111) surface state. The QWS's in the ARPES spectra were not discernible at the photon-energy range of 15–20 eV due to interference with the contribution from the second-order light of the beam line. In Fig. 7, the QWS peaks are clearly dispersive and show a cyclic or ''ratcheting'' behavior in their binding energies, as indicated by the thick lines. This phenomenon is very similar to that reported for the Ag(111) film on Ni(111).[25] The width of the peak shifts is roughly 0.3 eV but is slightly different for different QWS peaks. Each peak emerges from one end of the range of the shift, moves to the other end, pops back, and repeats its shift. Its intensity diminishes near the two ends of the shift, and reaches a maximum around the midpoint of that energy window. These energy positions with the intensity maxima are indicated by the thin solid lines in the figure. The intensity of the even-number QWS's is enhanced when that of the odd-number QWS's is reduced and vice versa. In clear contrast, the QWS peaks at $h\nu=20-25$ eV in Fig. 8 show no dispersion along the surface normal. Furthermore, there is no discernable difference in the appearance of the odd and even QWS's. The binding energies of the QWS peaks at $h\nu=20-25$ eV in Fig. 8 coincide with the midpoints of the energy window of the ratcheting QWS peaks at $h\nu=6-14$ eV in Fig. 7.

There have been a few ARPES studies that measured the photon-energy dependence of the QWS's of the Ag(111) films. Mueller, Miller, and Chiang performed a photoemission study of Ag(111)/Cu(111) at $h\nu=10$ and 11 eV.[24] No binding-energy shift was observed between these two photon energies. Evans and Horn[16] measured ARPES spectra of Ag(111)/GaAs(110) at $h\nu=32-57$ eV observing no dispersion with photon energy for the QWS peaks. They naturally attributed such little dispersion of both Ag(111)/Cu(111) (Ref. 24) and Ag(111)/GaAs(110) to the spatial confinement normal to the surface.[16] On the other hand, the ARPES study of Ag(111)/Ni(111) observed the QWS dispersion at $h\nu=5.5-13.75$ eV which is very similar to the present observation at $h\nu=5-14$ eV.[25] This behavior was interpreted as due to the limited spatial confinement of the QWS's through inevitable coupling to the substrate electronic states.[25] Such coupling leads to the broadening of the QWS energies in both initial and final states, causing the ratcheting peak positions of the corresponding ARPES peaks upon varying the photon energies.[25]

However at the first look, this interpretation seems to contradict the invariant QWS peak energies for higher photon energies, which was observed previously[16] and presently. This difference can be understood from the difference of the photoemission final states. The final states at the low-photon-energy range are the unoccupied Ag *sp* band, which disperse from 3 to 17 eV above E_F along the Γ-L line[36] and which are also quantized into the discrete states in the films.[20,21] In

contrast, at $E>16$ eV, above E_F the many unoccupied *d* bands can be the corresponding final states, which are almost continuum states with numerous quantum levels already at a coverage as thin as ~10 ML.[41] Thus, it is plausible to expect that the photoemission spectra of QWS's are distinguished into two types; the excitations into the discrete *sp*-band final states at <16 eV and those into the *d*-band continuumlike states at >16 eV. The observation of the ratcheting behavior at $h\nu=5.75-14.25$ eV is consistent with the above interpretation given previously and the lack of such behavior at higher photon energy is then explained by the lack of the discrete *sp* final states.

Within this interpretation a QWS is thought to have a finite energy width due to the coupling with the substrate bands. However, the $n=1$ QWS's of Ag(111)/Si(001) was also observed to disperse (Fig. 7), which is located obviously within the band gap of Si(001) and thus is expected to have no coupling to any substrate band.[30–31,42–44] This seems to suggest another mechanism for the energy-width broadening of a QWS. Although further study is required in this aspect, the QWS binding energy can uniquely be determined in an ARPES experiment by choosing the photon energy larger than ~16 eV avoiding the ratcheting behavior and can be compared to the theoretical calculations as in Figs. 5 and 6.

IV. CONCLUSIONS

The low-temperature growth and the electronic structures of the thin metastable Ag films on the Si(001)2×1 surface are investigated by STM and ARPES using synchrotron radiation. The as-deposited film at ~100 K is composed of 2D nanoclusters in a uniform quasi layer-by-layer film at 2–3 ML, which changes into the larger clusters having more 3D character at ~5 ML. These clusters possess a uniform size distribution of 20–30 Å and 30–40 Å at 2.5 and 5 ML, respectively. This morphology is altered drastically by a subsequent annealing at 300–450 K into two characteristically different structures. A percolating network of 2D islands of ~100 Å size is formed at 2.5 ML with rather disordered heights. In sharp contrast, atomically flat epitaxial Ag(111) films are formed at a nominal coverage larger than 5 ML. The growth morphology seems to be consistent with the recently introduced electronic-growth model of a magic thickness of 6 ML at high coverages. However, the discrepancy with this growth model is obvious at a lower coverage of 2.5 ML.

The ARPES spectra also exhibit a drastic change upon annealing. At the optimal annealing of 300–450 K, the epitaxial Ag(111) films of 6–30 ML are formed with the well-defined QWS of the Ag 5*s* band at binding energies of 0.3–3 eV together with the Ag(111) surface state. The surface state was shown to have more sensitivity for further annealing than the QWS. At higher annealing temperatures, the ARPES spectra gradually changes into that of the Si(001)2×3-Ag layer, which wets the surface after the Ag films coalesce into 3D islands. No such well-defined QWS is observed for the films with a coverage less than ~5 ML, which is most likely related to the different morphology at low coverage as observed by STM. The QWS's are consistently analyzed with the standard phase-shift quantization model. The phase shift of the QWS's at E_F in the Ag/Si interface is estimated to be close to π, indicating a far more perfect reflection of Bloch waves than an Ag/metal interface. The phase shift, the energy dispersion, and the thickness-versus-energy relation (the structure plot) of the QWS's of the epitaxial Ag(111) films are consistently derived. The QWS's in photoemission spectra show two distinctive types of the photon-energy dependence in their binding energies; the oscillatory shifts at $h\nu=5-15$ eV and no such shift at $h\nu=20-25$ eV, respectively. This can be explained in terms of the different final states in the photoemission process; the quantized *sp* band and the continuumlike *d* band for the lower and the higher binding-energy regimes, respectively.

ACKNOWLEDGMENTS

The authors are grateful to K. Horikoshi and S. Ouchi for their help during the STM experiments. I.M. gratefully acknowledges the financial support from High Energy Accelerator Research Organization through Professor A. Yagishita. H.W.T. was also supported by ASSRC of the Korean Science and Engineering Foundation and the BK21 program.

*Corresponding author. FAX: +82-2-312-7090. Email address: yeom@phya.yonsei.ac.kr

[1] R. M. Kolbas and N. Holonyak, Am. J. Phys. **52**, 431 (1984).
[2] R. C. Jaklevic and J. Lambe, Phys. Rev. B **12**, 4146 (1975).
[3] J. J. Paggel, T. Miller, and T.-C. Chiang, Science **283**, 1709 (1999).
[4] F. J. Himpsel, Science **283**, 1655 (1999).
[5] R. K. Kawakami, E. Rotenberg, E. J. Escorcia-Aparicio, H. J. Choi, T. R. Cummins, J. G. Tobin, N. V. Smith, and Z. Q. Qiu, Phys. Rev. Lett. **80**, 1754 (1998).
[6] F. J. Himpsel, Surf. Rev. Lett. **2**, 81 (1995).
[7] A. R. Smith, K.-J. Chao, Q. Niu, and C.-K. Shih, Science **273**, 226 (1996).
[8] G. Neuhold, L. Bartels, J. J. Paggel, and K. Horn, Surf. Sci. **376**, 1 (1997).
[9] L. Huang, S. J. Chey, and J. H. Weaver, Surf. Sci. **416**, L1101 (1998).
[10] G. Neuhold and K. Horn, Phys. Rev. Lett. **78**, 1327 (1997).
[11] M. H.-v. Hoegen, T. Schmidt, M. Henzler, G. Meyer, D. Winau, and K. H. Rieder, Phys. Rev. B **52**, 10 764 (1995).
[12] M. H.-v. Hoegen, T. Schmidt, M. Henzler, G. Meyer, D. Winau, and K. H. Rieder, Surf. Sci. **331-333**, 575 (1995).
[13] Z. Zhang, Q. Niu, and C.-K. Shih, Phys. Rev. Lett. **80**, 5381 (1998).
[14] L. Gavioli, K. R. Kimberlin, M. C. Tringides, J. F.Wendelken, and Z. Zhang, Phys. Rev. Lett. **82**, 129 (1999).
[15] D. A. Evans, M. Alonso, R. Cimino, and K. Horn, Phys. Rev. Lett. **70**, 3483 (1993).
[16] D. A. Evans and K. Horn, Surf. Sci. **307-309**, 321 (1994).
[17] M. Jalochowski, H. Knoppe, G. Lilienkamp, and E. Bauer, Phys. Rev. B **46**, 4693 (1992).
[18] F. Patthey and W.-D. Schneider, Phys. Rev. B **50**, 17 560 (1994).

[19] A. L. Wachs, A. P. Shapiro, T. C. Hsieh, and T.-C. Chiang, Phys. Rev. B **33**, 1460 (1986).
[20] J. E. Ortega, F. J. Himpsel, G. J. Mankey, and R. F. Willis, Surf. Rev. Lett. **4**, 361 (1997).
[21] J. E. Ortega, F. J. Himpsel, G. J. Mankey, and R. F. Willis, Phys. Rev. B **47**, 1540 (1993).
[22] N. V. Smith, Phys. Rev. B **49**, 332 (1994).
[23] J. J. Paggel, T. Miller, and T.-C. Chiang, Phys. Rev. B **61**, 1804 (2000).
[24] M. A. Mueller, T. Miller, and T.-C. Chiang, Phys. Rev. B **41**, 5214 (1990).
[25] T. Miller, A. Samsavar, and T.-C. Chiang, Phys. Rev. B **50**, 17 686 (1994).
[26] St. Tosch and H. Neddermeyer, Phys. Rev. Lett. **61**, 349 (1988); H. Neddermeyer, Crit. Rev. Solid State Mater. Sci. **16**, 309 (1990).
[27] K. Tsuchie, T. Nagao, and S. Hasegawa, Phys. Rev. B **60**, 11 131 (1999).
[28] H. Namba, M. Masuda, H. Kuroda, T. Ohta, and H. Noda, Rev. Sci. Instrum. **60**, 1917 (1989).
[29] F. Matsui, H. W. Yeom, I. Matsuda, and T. Ohta, Phys. Rev. B **62**, 5039 (2000).
[30] H. W. Yeom, I. Matsuda, K. Tono, and T. Ohta, Phys. Rev. B **57**, 3949 (1998).
[31] I. Matsuda, H. W. Yeom, K. Tono, and T. Ohta, Phys. Rev. B **59**, 15 784 (1999).
[32] I. Matsuda, H. W. Yeom, K. Tono, and T. Ohta, Surf. Sci. **438**, 231 (1999).
[33] S. M. Shivaprasad, T. Abukawa, H. W. Yeom, M. Nakamura, S. Suzuki, S. Sato, K. Sakamoto, T. Sakamoto, and S. Kono, Surf. Sci. **344**, L1245 (1995).
[34] G. Meyer and K. H. Rieder, Appl. Phys. Lett. **64**, 3560 (1994); Surf. Sci. **331–333**, 600 (1995).
[35] Z. H. Zhang, S. Hasegawa, and S. Ino, Phys. Rev. B **55**, 9983 (1997).
[36] H. Wern, R. Courths, G. Leschik, and S. Hufner, Z. Phys. B: Condens. Matter **60**, 293 (1985).
[37] A. Beckmann, M. Klaua, and K. Meinel, Phys. Rev. B **48**, 1844 (1993).
[38] E. G. McRae and M. L. Kane, Surf. Sci. **108**, 435 (1981).
[39] J. Holzl, F. K. Schulte, and H. Wagner, *Solid Surface Physics*, Springer Tracts in Modern Phys. Vol. 85 (Springer-Verlag, Berlin, 1979).
[40] W. E. McMahon, T. Miller, and T.-C. Chiang, Phys. Rev. B **54**, 10 800 (1996).
[41] D.-A. Luh, J. J. Paggel, T. Miller, and T.-C. Chiang, Phys. Rev. Lett. **84**, 3410 (2000).
[42] L. S. O. Johansson, R. I. G. Uhrberg, P. Martensson, and G. V. Hansson, Phys. Rev. B **42**, 1305 (1990).
[43] H. W. Yeom, T. Abukawa, Y. Takakuwa, M. Nakamura, M. Kimura, A. Kakizaki, and S. Kono, Surf. Sci. Lett. **321**, L177 (1994).
[44] H. W. Yeom, T. Abukawa, Y. Takakuwa, Y. Mori, T. Shimatani, A. Kakizaki, and S. Kono, Phys. Rev. B **53**, 1948 (1996).